

Statistical Re-examination of Reported Emission Lines in the X-ray Afterglow of GRB 011211

Robert E. Rutledge¹ and Masao Sako^{1,2}

ABSTRACT

A 0.2-12 keV spectrum obtained with the *XMM-Newton* EPIC/pn instrument of GRB 011211, taken in the first 5 ksec of a 27 ksec observation, was found by Reeves et al. (2002) to contain emission lines which were interpreted to be from Mg XI, Si XIV, S XVI, Ar XVIII, and Ca XX, at a lower-redshift ($z_{obs} = 1.88$) than the host galaxy ($z_{host} = 2.14$). We examine the spectrum independently, and find that the claimed lines would not be discovered in a blind search. Specifically, Monte Carlo simulations show that the significance of reported features, individually, are such that they would be observed in 10% of featureless spectra with the same signal-to-noise. Imposing a model in which the two brightest lines would be Si XIV and S XVI $K\alpha$ emission possibly velocity shifted to between $z=1.88-2.40$, such features would be found in between $\sim 1.2\text{--}2.6\%$ of observed featureless spectra. We find the detection significances to be insufficient to justify the claim of detection and the model put forth to explain them. $K\alpha$ line complexes are also found at $z = 1.2$ and $z = 2.75$ of significance equal to or greater than that at $z = 1.88$. Thus, if one adopts the $z = 1.88$ complex as significant, one must also adopt the other two complexes to be significant. The interpretation of these data in the context of the model proposed by R02 is therefore degenerate, and cannot be resolved by these data alone. Our conclusions are in conflict with those of Reeves et al., because our statistical significances account for the multiple trials required – but not accounted for by Reeves et al. – in a blind search for emission features across a range of energies.

Subject headings: gamma rays: bursts — gamma rays: observations

¹ Theoretical Astrophysics, California Institute of Technology, MS 130-33, Pasadena, CA 91125; rutledge@tapir.caltech.edu, masao@tapir.caltech.edu

² Chandra Fellow

1. Introduction

It was recently reported that the X-ray afterglow of gamma-ray burst GRB 011211, as observed with *XMM-Newton* EPIC/pn, contained spectral emission lines (Reeves et al. 2002, hereafter, R02) – the first report of multiple X-ray emission lines from a GRB. These lines, at 0.45, 0.70, 0.89, 1.21, and 1.44 keV were interpreted to be from He-like Mg XI (rest energy 1.35 keV) and H-like Si XIV(2.0 keV), S XVI (2.62 keV), Ar XVIII (3.32 keV) and Ca XX (4.10 keV), redshifted to $z=1.88$. The difference between this and the known redshift of the host galaxy $z_{host} = 2.14$ was modeled as due to supernova ejecta traveling at $v = 25800 \pm 1200 \text{ km s}^{-1}$, which had originated during a supernova 4 days prior to when the GRB jet illuminated it, producing the afterglow.

The statistical significance of the individual lines was not reported in R02; it was stated that joint analysis of the lines taken together produced an improvement in the χ^2 value which, by an F-test, yielded a significance level of 99.7%. In addition, it was found that Monte Carlo (MC) simulations were unable to produce the same improvement in χ^2 found between the best-fit power-law model and the best-fit five emission-line model more than 0.02% of the time. Specifically, it was found that the best-fit χ^2 value for a power-law model was improved by fitting to a model of a MEKAL plasma with emission lines at rest energies corresponding to unresolved Mg XI, Si XIV, S XVI, Ar XVIII, and Ca XX redshifted to $z = 1.88$ in only 0.02% of the simulated spectra (a 99.98% confidence detection).

The implications of the model discussed by R02 – a delay between a supernova and a GRB on a timescale of days, the formation of a thin shell of supernova ejecta, an apparent under-abundance of Fe relative to the detected nuclei – provide severe constraints on gamma-ray burst emission models. In addition, as demonstrated by R02, the future detection of multiple emission lines can provide extremely strong constraints on the production mechanisms, due to the inherent required outflow velocity and emission timescales which can be derived from them, not to mention the implied association with supernovae. Similar spectra observed with greater S/N in the future would greatly aid in unravelling the emission mechanisms and geometry of gamma-ray bursts. Therefore, it is of wide theoretical (e.g. Lazzati et al. 2002; Kumar & Narayan 2002) and observational interest to further interpret the observed X-ray spectrum of this GRB 011211, in hopes of determining what more could be learned from future, more precise observations.

In Sec. 2, we describe the observation, and perform a basic spectral analysis using continuum models. In Sec. 3, we compare Monte Carlo (MC) realizations of acceptable continuum models with the GRB spectrum, and find that the reported features would be produced in $\sim 10\%$ of the continuum model spectra, due only to Poisson noise. In Sec. 4, we adopt the model that the two apparently most significant lines are K α lines of Si XIV and

S XVI; we perform a blind search for features of the same significance in MC realizations of continuum spectra, and find that they would be reported from \sim 1.2-2.6% of such spectra, again, due only to Poisson noise. We conclude in Sec. 5 that the lines are not individually significant in the absence of an imposed model, and are only marginally significant when the adopted model is imposed.

These conclusions conflict with those of R02. R02 derived the model (that is, the observed line energies, or redshifts) from the data, and then applied statistics for detection as if the energies were known prior to examining the data (that is, single-trial statistics). This is not appropriate when the model line energies are derived directly from the X-ray data, and not from an *a priori* model – one derived without examination of the X-ray data (for example: line energies of multiple features with redshifts of the host galaxy). We adopt statistics appropriate to a blind-search for these features, across a range of energies or redshifts (multi-trial statistics). This accounts for the diminished significance we find for the features. We further discuss the reasons for this conflict and conclude in § 5.

2. Observation and Observed Spectrum

We analyzed the identical source and background *XMM-Newton*/EPIC-pn (Strüder et al. 2001) spectrum as used by R02 (their Fig. 2), which was kindly made available to us by the authors in electronic form (J. Reeves, priv. comm.). We used the same response matrix (`epn_ff20_sdY9_thin.rsp`). The spectrum used 5000 sec of realtime observation beginning at 07:14:33 UT on 12 Dec 2001, with a total live time of 4440 sec. The pn spectrum used counts comprised of grades 0–4 (singles and doubles), from a circular region 46'' in radius centered on the source, excluding flagged events (for which the keyword `FLAG!=0`) and excluding a region near the edge of the CCD chip.

We performed a basic spectral analysis using XSPEC v11.1.0 (Arnaud 1996). We used data in the 0.2–12 keV energy range. We performed a non-standard spectral binning, implemented to maximize the signal-to-noise associated with the reported emission features at the reported energies. We first binned data with energy bins centered at the five best-fit line energies found by R02, with bin-sizes approximately equal to the FWHM EPIC/pn energy response at each energy (respectively: 62 eV, 66 eV, 68 eV, 72 eV and 75 eV; see Eq. 1). The remaining data were binned with 60 eV or greater (< 1 keV), and 70 eV or greater (> 1 keV).

We fit an absorbed power-law spectrum to the data, shown in Fig. 1. The model spectrum was statistically acceptable (model parameters are listed in Table 1, along with

the obtained χ^2 values). We also fit the model with a thermal bremsstrahlung spectrum (`wabs*brems`), and derived an acceptable best fit. Finally, we found best-fit model parameters for the values of the power-law photon slope (models 2 and 3) and kT_{brems} (models 5 and 6) at the 90% confidence limits of the best-fit, which will be used in MC simulations in § 3.

3. Individual Emission Line Significances

We first determine which of the reported lines are individually statistically significant, when one is searching for emission lines at *a priori* known energies. We compared the observed spectrum with MC simulations of six featureless spectra – the three absorbed power-law and three absorbed thermal bremsstrahlung which are models 1-6 in Table 1.

We used a “matched filter”, convolving the observed pulse-invariant (PI) counts spectrum with a Gaussian energy response, with the energy resolution response of the detector. The matched filter approach maximizes the signal-to-noise ratio as a function of energy of unresolved lines in the X-ray PI spectrum.

Based on Figure 18 in *XMM-Newton* v1.1 POG, we modelled the photon energy redistribution as a Gaussian response, with FWHM:

$$FWHM(E) = 57 + 13(E/1\text{keV}) - 0.29(E/1\text{keV})^2 \text{ eV} \quad (1)$$

We performed a convolution between the raw PI spectrum (that is, number of counts vs. PI bin) and the gaussian energy response function, as a function of energy:

$$C(E_i) = \sum_{j(E_i-3\sigma(E_i))}^{j(E_i+3\sigma(E_i))} I(j) \frac{1}{\sqrt{2\pi}\sigma(E_i)} \exp^{-\frac{1}{2}\left(\frac{E_i-E_j}{\sigma(E_i)}\right)^2} \delta E_j \quad (2)$$

where N is the number of PI bins, and we sum across PI bins which are within $\pm 3\sigma(E_i)$ of E_i . The centroid (average) energies and energy widths (ΔE_j) of the PI bins were taken from the EBOUNDS extension of the response matrix, where i is the PI bin number and $\sigma(E) = FWHM(E)/2.35$. We do not correct the PI spectrum for the detector area; however the detector area does not change dramatically across the FWHM of the lines. If the area did change dramatically across the FWHM of a line, and a statistical excess were observed in the area-corrected PI spectrum but not in the raw PI spectrum, then such an excess could well be due to calibration uncertainties.

The resulting $C(E_i)$ is shown in Fig. 2a. By visual inspection, there are indeed features in the spectrum near energies where the reported lines occur.

To determine if these features are significant, we produced MC spectra of models 1-6 (see § 2). The MC realizations of the raw PI spectra were performed as follows. We simulated the spectral models 1-6 in XSPEC, using the same response matrix as above, so that the resulting PI spectra (without Poisson noise added) were convolved as the observed spectrum through the telescope and detector response. The simulated PI spectra $N(E)$ each had a total of $>9\times10^8$ counts in PI bins between 0.2-3 keV. We then produced integrated spectra $I(E) = \int_{0.2\text{ keV}}^E N(E) dE / \int_{0.2\text{ keV}}^{3\text{ keV}} N(E) dE$, so that $I(0.2\text{ keV}) = 0$ and $I(3\text{ keV}) = 1$ (the integrated normalized model is used for the MC simulation as described below). These constitute our six acceptable featureless spectral models; we will compare the data with results from all six, as a firm conclusion that emission lines are present should be independent of the underlying broad-band model assumed.

We implemented a background spectral model, to simulate the $\sim 10\%$ of the counts due to background. Taking background from a different part of the detector, we find that it can be parameterized by a broken photon power-law (**bknpower**), with $\alpha_1 = 2.4$ at low energies, break energy 1.35 keV, and $\alpha_2 = 0.44$ at high energies, between 0.20-7.3 keV (there is a strong background line at 8 keV). In fact, there are statistically significant deviations from this pure continuum model between 0.55-0.6 keV; we ignore these deviations in our background model. In our MC simulation the effect of ignoring what would appear to be a line in the observed spectrum is conservative, in the sense that by ignoring its presence in the background model, we could detect as “significant” a line in the 0.55-0.6 keV range which is in fact produced by instrument background.

We simulated spectra between 0.2 and 3 keV, in which there were 560 counts observed, of which we estimate ~ 66 counts are due to background; this is identical to the number of total counts observed and our estimate for the number of these counts which are due to background. We drew, for each MC realization, 494 counts from the MC source spectral model and 66 from our background spectral model. To produce a simulated spectrum, we generate a random uniform deviate r between 0 and 1, and we place a count in the PI bin in which $I(E) = r$.

To produce our 99% confidence limit to $C(E)$, we produced 167 MC realizations each of models 1-6 for a total of 1002 realizations; we set the 99% confidence limit at the 10th greatest value of $C(E)$ of all such realizations. We similarly produce 1667 MC realizations each of models 1-6 for a total of 10002 realizations, using the 10th greatest values $C(E)$, to produce our 99.9% confidence limit. This insures that the conclusions are not dependent upon the assumed featureless spectral model.

The results of this MC simulation are shown in Fig. 2a. Two of the reported features (near 0.7 keV and 0.85 keV; Si XIV and S XVI) have single-energy-trial probabilities of 99% and 99.9% confidence, respectively, in comparison with the featureless spectral models. The remaining three lines are not significant in comparison with single-energy-trial probability of 99% confidence.

In Fig. 2, we also show $C(E)$ for single MC realizations of the best-fit power-law spectrum (model 1), which also contain apparent features. The bumps in the single simulated spectra appear because in any spectrum which contains Poisson noise, the counts will not be distributed uniformly in energy, but will be clustered in energy simply due to counting statistics.

3.1. Multi-Energy-Trial (Blind Search) Probabilities

Since it was necessary to perform a blind-search for emission line features in the GRB spectrum – as the redshifted line energies were not known *a priori*, but were measured from the data – it is necessary to estimate the chance probability that the reported features are produced from a featureless spectrum during a blind search for such features.

We produced 10000 MC realizations for each of models 1-6 as described in the previous section. We compared the $C(E)$ of these between 0.4 and 1.5 keV against the single-energy-trial 99% and 99.9% confidence limits we found in the previous section, for the models 1-6 individually.

In Table 2 we list the fraction of the 10000 MC spectra in which $C(E)$ in at least one PI bin reaches a single-energy-trial probability of 99% or 99.9% confidence. These fractions are 77-82% and 14-16%, respectively; if finding a single-energy-trial 99% and 99.9% feature were statistically independent, then the probability of observing both a 99% and 99.9% single-energy-trial “line” in a single spectrum, such as we find in the present spectrum of GRB 011211, is $\approx 10\%$.

Therefore, in a blind-search of the EPIC/pn spectrum for emission features, we would expect to find features which have single-energy-trial significance equal or greater to those observed in one of approximately ten observed featureless spectra.

4. Line Complex Significance As a Function of Redshift

In this section, we examine if the reported lines, taken together, implicate K α emission features from the particular redshift of $z=1.88$ as reported by R02. We do so by summing the $C(E_i/(1+z))$, using the values of the rest energies of the reported lines:

$$\chi(z) = \sum_i^{N_{\text{lines}}} \sum_j^N I(j) \frac{1}{\sqrt{2\pi}\sigma(E_j)} \exp -\frac{1}{2} \left(\frac{E_j - (E_{\text{line},i})/(1+z)}{\sigma(E_j)} \right)^2 \quad (3)$$

$$(4)$$

where j denotes the PI bin number, E_j is the centroid energy of the j th PI bin, i denotes the index [1, 5] of the five lines reported detected; E_i denotes the rest energies of the five lines identified by R02, which were 1.35 (Mg XI), 2.00 (Si XIV), 2.62 (S XVI), 3.32 (Ar XVIII), and 4.10 keV (Ca XX). We examined the range of $0 < z < 3$, with a step-size of $\Delta z = 0.015$. We use PI bins with energies 0.1-7 keV, to cover the spectrum past the rest frame energy of Ca XX. We find 638 counts in this energy range, of which we estimate 80 are from background. We use only bins which are within $3\sigma(E_i/(1+z))$ of each $E_i/(1+z)$. The result of this convolution, if the reported lines are real, should be a maximum in $\chi(z)$ near the optimal redshift value, in excess of that found from MC realizations of data with featureless spectra.

The average value of χ will systematically increase with increasing z as the lines are shifted to lower energies, where the the intensity is higher in the power-law spectrum and the detector effective area is larger and so there are a greater number of counts. To examine if any particular maximum in $\chi(z)$ is significant, we performed this convolution for 1000 and 10000 MC realizations using the simulated spectral models 1-6, as described in the previous section, to produce the 99% and 99.9% confidence limits.

The results of the calculation using all 5 reported lines, as well as the 99% and 99.9% MC confidence limits, are in Fig. 3. The value of $\chi(z)$ is in excess of the 99% MC confidence limit at $z = [1.88 - 1.95]$ (6 z bins wide), and in excess of the 99.9% MC confidence limit at $z = [2.70 - 2.79]$.

We also performed this convolution and Monte-Carlo simulation using what appear to be the most significant two lines from Fig.2 of R02 (Si XIV and S XVI), the results of which are also shown in Fig. 3. The value of $\chi(z)$ is in excess of the 99.9% MC confidence limit at $z = [1.88 - 1.95]$, and in excess of the 99% MC confidence limit at $z = [1.155 - 1.245]$.

4.1. Multi-Redshift-Trial (Blind Search) Probabilities

What fraction of featureless spectra, with the same number of source and background counts as the observed spectrum, would produce values of $\chi(z)$ of comparable significance to the excess in $\chi(z = 1.88)$ from the observed spectrum? If one examines $\chi(z)$ only at $z = 1.88$, the answer is <1%, which is the single- z -trial probability. However, the reported $z = 1.88$ is different from the known redshift of the host galaxy $z = 2.14$; it is therefore unlikely that $z = 1.88$ was the only redshift which would be considered consistent with an *a priori* model by R02. The pertinent statistical question to ask, then, is what is the fraction of featureless X-ray spectra, examined for a redshifted pair of S XVI and Si XIV lines, would produce a value of $\chi(z)$ comparable to the single- z -trial significance observed, allowing for a blind-search at values of z between 1.88 and 2.40 (a range of equal magnitude redshift and blueshift from the host galaxy)?

To address this, we simulated 10000 MC spectra of each of spectral models 1-6, and found $\chi(z)$ in the same way as for the observed spectrum in the previous section. We used only the 2-line model, as this gave the apparently most significant result near $z = 1.88$. We compared $\chi(z)$ with the 99% and 99.9% MC limits, found in the previous section, and noted when these were exceeded in at least one z bin for the 99% confidence limit, and in at least six consecutive z bins for the 99.9% confidence limit (as was observed) between $z = 1.88$ and $z = 2.40$.

The fraction of MC featureless spectra which contained at least one z bin between $z = 1.88$ and $z = 2.40$ in excess of the single- z -trial MC probability of 99% are given in Table 3. Because the observed spectrum gave $\chi(z) > 99.9\%$ in six consecutive z bins, we also used this as our criterion to count “hits” in the >99.9% confidence comparison, also shown in Table 3. Of 10000 MC spectra, between 16-25% exceed a single- z -trial 99% confidence limit, and 1.2-2.6% exceed a single- z -trial 99.9% confidence limit in six (or more) consecutive z bins.

We note that if we search in the range $z = 2.14 \pm 0.5$ (instead of ± 0.26) and require only a “single” z -bin hit, the percentage of featureless spectra which have one bin with $\chi(z) > 99.9\%$ is 2.2-3.7%. Thus, the model-dependent interpretation of the reported lines is of marginal significance.

5. Discussion and Conclusion

We have attempted to confirm the observational statistical significance of emission lines in the X-ray afterglow of GRB 011211. In a blind-search for individual emission lines

between 0.4 and 1.5, features of significance equal to those observed will be found in one in ten featureless spectra. Thus, the reported features can be said to be detected with 90% confidence in a model-independent way.

Also, a blind-search for the two-line complex (Si XIV and S XVI) at any redshift between the reported value ($z = 1.88$) and a blueshift of equal magnitude from the host galaxy ($z = 2.40$) would find such features with equal significance to that observed in 1 of 40 featureless spectra (1.2-2.6% of the time, depending on the intrinsic spectrum). Thus, the features as reported can be said to be detected with 97.4-98.8% confidence, in a model-dependent interpretation, where we search for two features due to Si XIV and S XVI K α redshifted to some value of z in the range $z = 2.14 \pm 0.26$.

The difference between the present statistics and those of R02 are due to the different statistical arguments used to establish the existence of the emission lines. While R02 relies on single-trial statistics, we find the model used by R02 (K α lines, at a redshift different from that of the host galaxy) was derived directly from the data, which therefore requires a statistical analysis appropriate to a blind search. By expanding the searched phase-space, and taking into account the multiple trials of a blind search, the confidence in the detection drops from the 99.98% of R02 to, the 98.8% (best case) we find here. Moreover, R02 did not estimate the individual significances of the lines as we do here; thus we find that such “lines” would appear in $\approx 75\%$ (for a significance comparable to that of the reported Si XIV line) and $\approx 15\%$ (for a significance comparable to that of the reported S XVI line) of featureless continuum spectra.

The analysis of these data has otherwise recently been called into question. Borozdin & Trudolyubov (2002) have shown that there is a background line associated with the EPIC/pn detector edge during the observation, which would have been included in the GRB spectrum from the first 5 ksec, when the source was near the detector edge, but not afterwards, after the source had been moved away from the detector edge. In our own analysis, we cannot confirm this result unless we adopt non-standard event selection criteria, which differ from the ones used by R02. R02 removed events near the CCD detector edge (**FLAG==0**) and selected only single and double events (**PATTERN<=4**) (J. Reeves, priv. comm.). These selections result in a smooth, featureless background spectrum with no bright line-like feature near ~ 0.7 keV (as seen in Fig. 4f of Borozdin & Trudolyubov 2002) as well as a reduction of the count rate by a factor of $\gtrsim 2$ in the range $E = 0.2 - 3$ keV (see Fig. 4). Therefore, we are not able to confirm the applicability of (Borozdin & Trudolyubov 2002) to the analysis of R02.

We consider neither a 90% confidence detection in a model-independent interpretation, nor a 97.4-98.8% confidence detection in a model-dependent interpretation, to be sufficient

to justify the detection claims and subsequent interpretation put forth by R02.

Moreover, if one concludes that the marginal detection of the 2 lines (Si & S) near $z = 1.88$ is significant, then one must also conclude that the detection of all 5 lines near $z = 2.75$ is equally significant. In addition, if one concludes that the marginal detection of the 5 lines near $z = 1.88$ is significant, then one must also conclude that the detection of 2 lines (Si & S) near $z = 1.2$ is equally significant.

Therefore, one cannot conclude simply that a complex of $K\alpha$ line emission is detected near $z = 1.88$; these data permit alternate interpretations of such complexes near $z = 1.2$ and $z = 2.75$. As the statistical excesses are due to the same “features” in the observed spectrum, the interpretation of the statistical excess in the context of the model presented by R02 is degenerate and cannot be resolved with these data alone.

Prospects for confirmation of line features in GRBs are very good, considering that the X-ray spectral integration for GRB 011211 was begun 11 hours after the GRB was initially detected, and required 1.4 hrs of integration to obtain. Decreasing the reaction time would permit a longer integration, while the afterglow is brighter in the X-rays, and the marginal results found here may well be improved upon.

We are grateful to J. Reeves, who generously made his observed spectrum of the first 5 ksec of the *XMM-Newton* observation of GRB 011211 available to us, that we might independently analyze it. We gratefully acknowledge useful conversations with A. MacFadyen, R. Blandford, and D. Fox. The authors are grateful to F. Harrison and F. Paerels for useful comments on the manuscript. MS was supported by NASA through *Chandra* Postdoctoral Fellowship Award Number PF1-20016 issued by the *Chandra* X-ray Observatory Center, which is operated by the Smithsonian Astrophysical Observatory for and behalf of NASA under contract NAS8-39073.

References

- Arnaud, K. A., 1996, in G. Jacoby & J. Barnes (eds.), *Astronomical Data Analysis Software and Systems V.*, Vol. 101, p. 17, ASP Conf. Series
- Borozdin, K. N. & Trudolyubov, S. P., 2002, ApJ, submitted, astro-ph/0205208
- Kumar, P. & Narayan, R., 2002, ApJ, submitted, astro-ph/0205488
- Lazzati, D., Ramirez-Ruiz, E., & Rees, M. J., 2002, ApJ 572, L57
- Reeves, J. N., Watson, D., Osborne, J. P., Pounds, K. A., O’Brien, P. T., Short, A. D. T., Turner, M. J. L., Watson, M. G., Mason, K. O., Ehle, M., & Schartel, N., 2002, Nature

416, 512

Strüder, L., Briel, U., Dennerl, K., Hartmann, R., Kendziorra, E., Meidinger, N., Pfeffermann, E., Reppin, C., Aschenbach, B., Bornemann, W., Bräuninger, H., Burkert, W., Elender, M., Freyberg, M., Haberl, F., Hartner, G., Heuschmann, F., Hippmann, H., Kastelic, E., Kemmer, S., Kettenring, G., Kink, W., Krause, N., Müller, S., Oppitz, A., Pietsch, W., Popp, M., Predehl, P., Read, A., Stephan, K. H., Stötter, D., Trümper, J., Holl, P., Kemmer, J., Soltau, H., Stötter, R., Weber, U., Weichert, U., von Zanthier, C., Carathanassis, D., Lutz, G., Richter, R. H., Solc, P., Böttcher, H., Kuster, M., Staubert, R., Abbey, A., Holland, A., Turner, M., Balasini, M., Bignami, G. F., La Palombara, N., Villa, G., Buttler, W., Gianini, F., Lainé, R., Lumb, D., & Dhez, P., 2001, *A&A* 365, L18

Fig. 1.— **(Top Panel)**: X-ray spectrum from *XMM-Newton* EPIC/pn of GRB 011211, with energy binning optimized to find deviations from the best-fit power-law spectrum (solid line) due to emission lines at the reported energies, with a best-fit absorbed power-law model. The data show no significant excess counts at the reported line energies. **(Bottom Panel)**: $\chi = (\text{model-data})/\sigma$, residuals between the best-fit continuum spectra and the data.

Fig. 2.— **(Panel a)**: Solid line is $C(E)$ (Eq. 2) from the observed raw PI spectrum – the convolution between the raw spectrum and the EPIC/pn energy response. The broken lines are the $\text{max}(C(E))$ for spectral models 1-6, showing the 99% and 99.9% confidence single-trial upper-limits. **(panels b-f)**: The dotted line is the same observed convolved spectrum as in Panel a. Solid lines are five (in the five separate panels) randomly selected Monte Carlo spectra using Model 1. Features of similar magnitude to those found in the observed spectra are apparent in each; these are due to the Poisson noise distribution (in energy) in a spectrum with a finite number of detected counts.

Fig. 3.— **(Top panel)** Figure of merit $\chi(z)$ using all five reported line energies (solid line), for $0 < z < 3$. We also show the extremum Monte-Carlo values for 99% (long dashed) and 99.9% confidence (short dashed), using all six model spectra. The solid vertical line marks the redshift of the reported detection ($z=1.88$); at this redshift, the $\chi(z = 1.88)$. **(Bottom Panel)** Same, except for only Si XIV and S XVI lines. Again, there $\chi(z = 1.88)$ is below 99% confidence limit.

Fig. 4.— The background spectrum near the region near the CCD chip edge using two different event selection criteria. (a) no explicit selection of **PATTERN** and **FLAG** as adopted by Borozkin & Trudolyubov (2002) (circles) and (b) using only **PATTERN** \leq 4 and **FLAG**=0 events as adopted by R02 (stars).

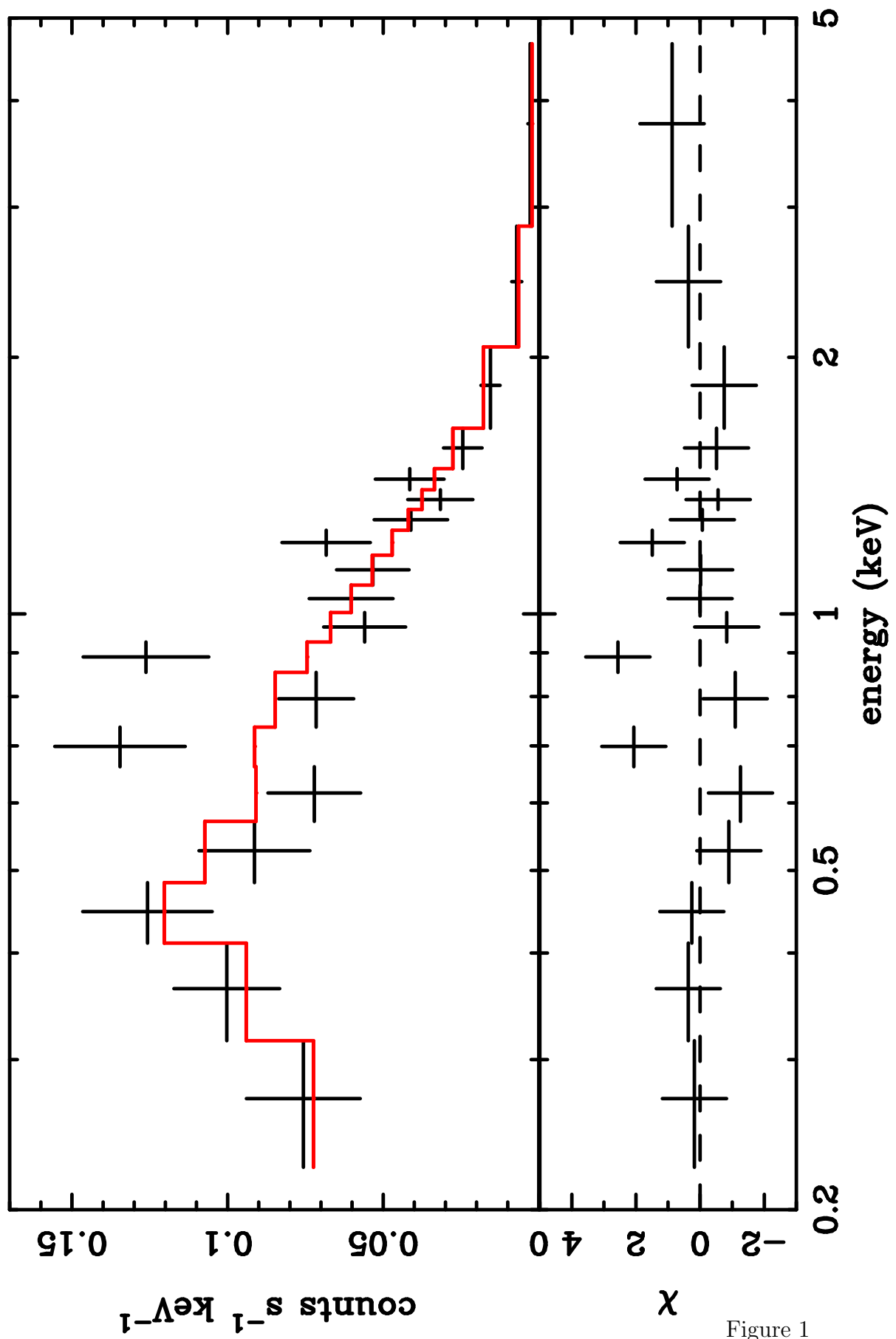


Figure 1

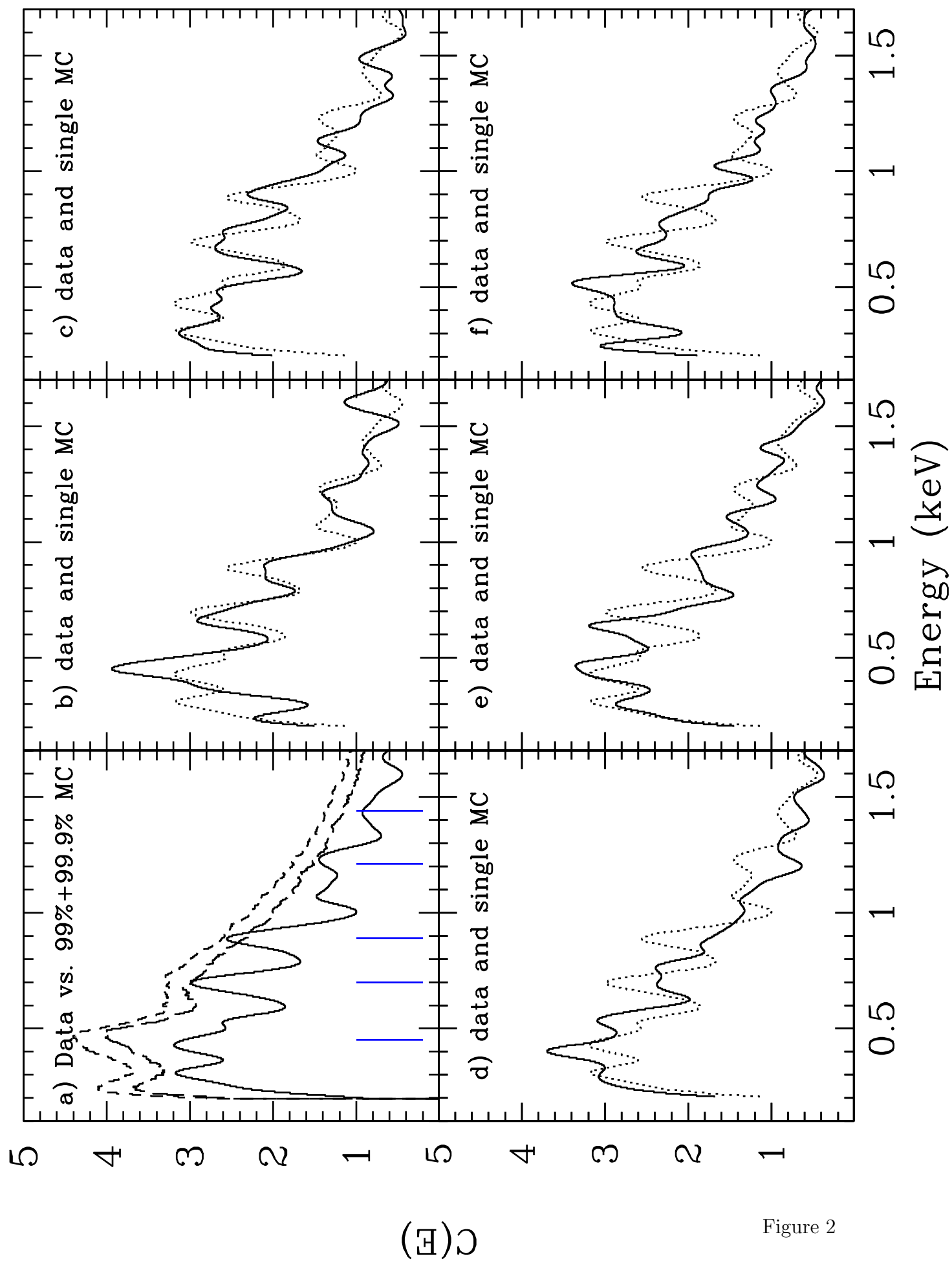


Figure 2

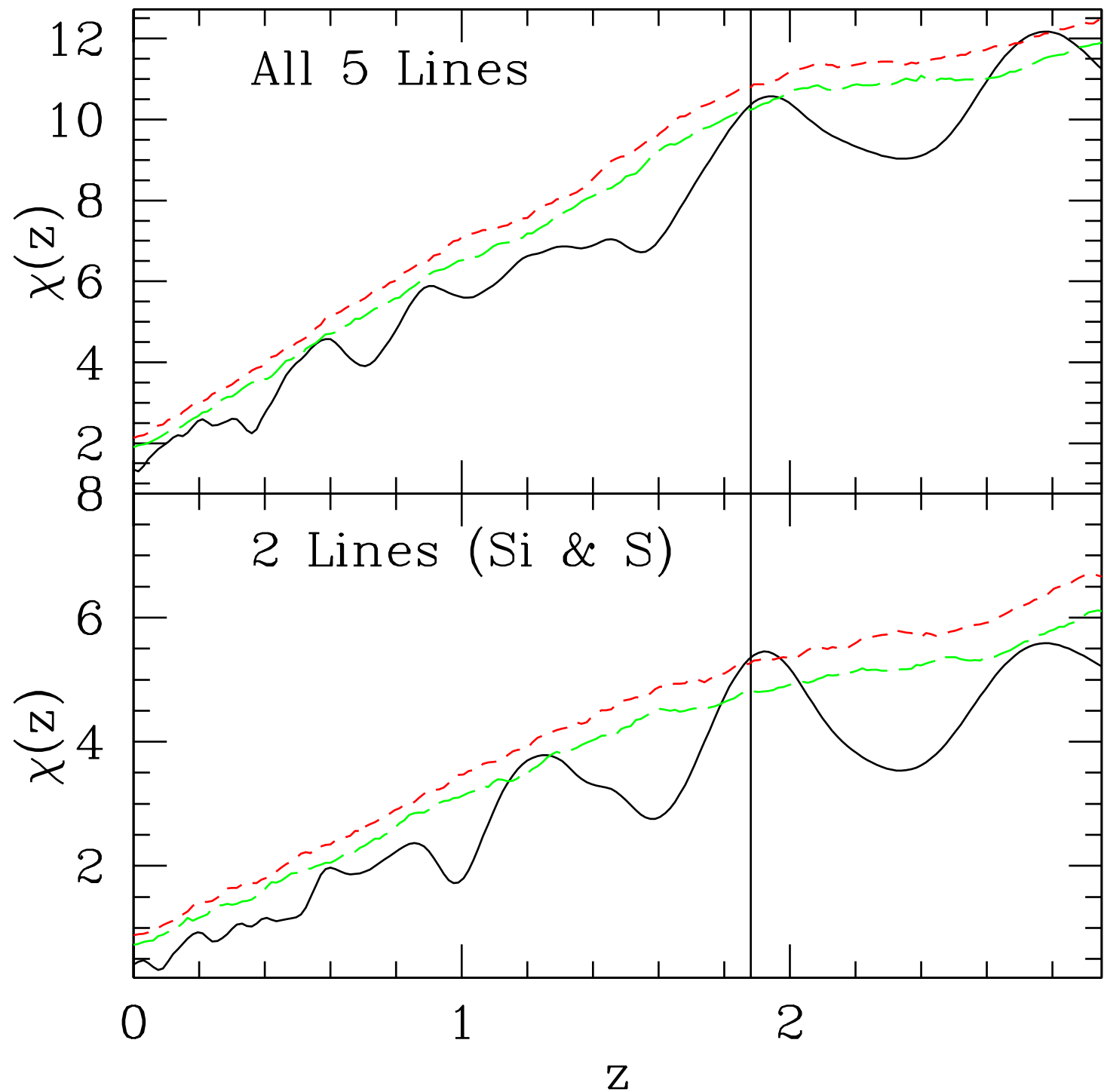


Figure 3

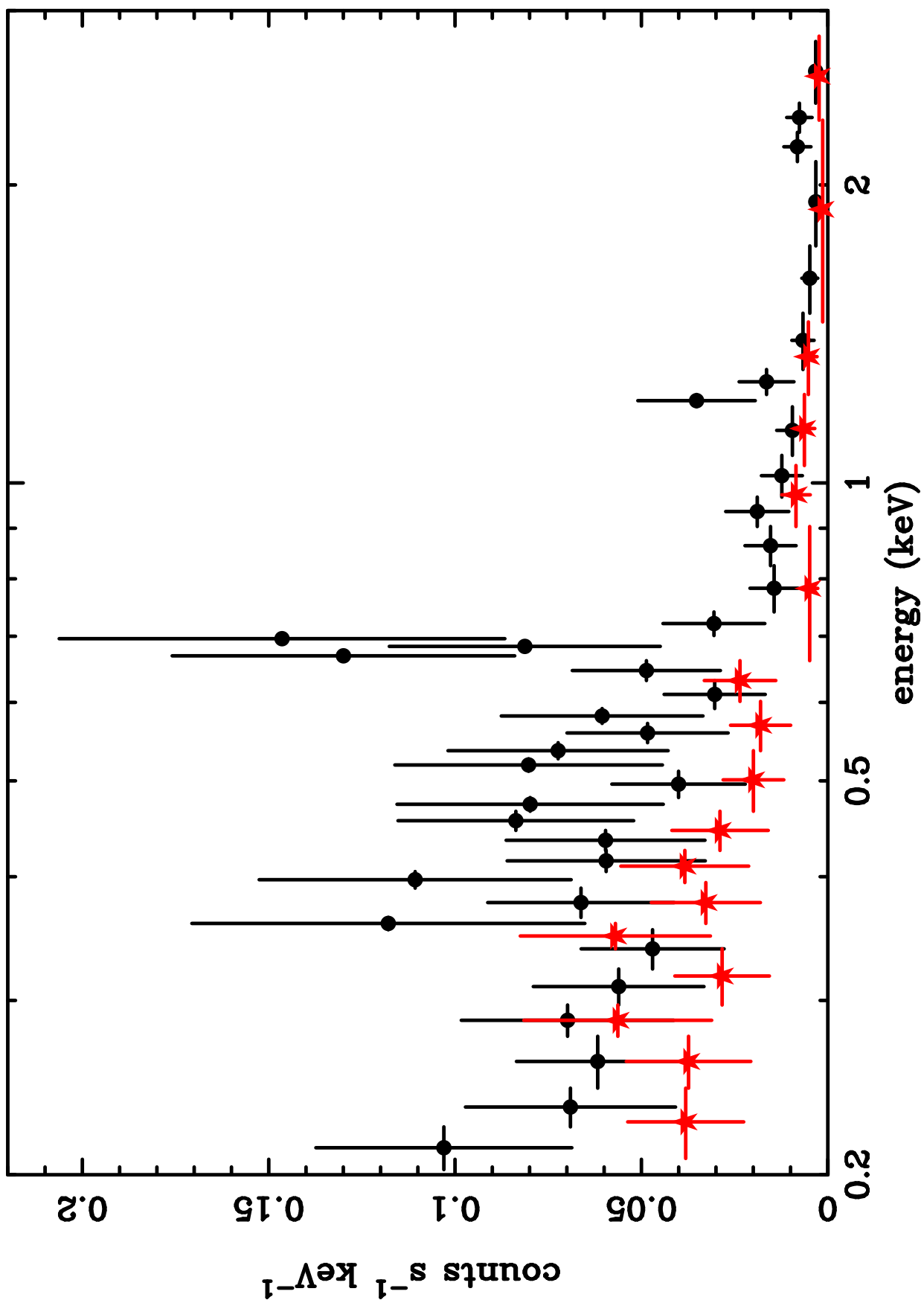


Figure 4

Table 1. Best-fit X-ray Spectral Parameters

Model	N_{H} (10^{22} cm^{-2})	$\alpha/kT_{\text{bremss}}$	N phot/keV/cm 2 /s at 1 keV	χ_{ν}^2/dof (prob)
(1) Best Fit	$0.10^{+0.04}_{-0.02}$	2.6 ± 0.2	$(6.9 \pm 0.9) \times 10^{-5}$	1.24/22 (0.20)
2	0.065 ± 0.01	(2.3)	$(5.8 \pm 0.05) \times 10^{-5}$	1.31/23 (0.09)
3	0.16 ± 0.02	(3.0)	$(8.5^{+0.6}_{-1.0}) \times 10^{-5}$	1.32/23 (0.14)
Thermal Bremsstrahlung				
(4) Best Fit	0.03 ± 0.01	$1.5^{+0.4}_{-0.2}$	$(9.0 \pm 1.2) \times 10^{-5}$	1.32/22 (0.14)
5	0.05 ± 0.01	(1.1)	$(12 \pm 1) \times 10^{-5}$	1.40/23 (0.10)
6	$0.014^{+0.009}_{-0.008}$	(2.1)	$(7.4 \pm 0.4) \times 10^{-5}$	1.38/23 (0.11)

Note. — Parameters in parenthesis were held fixed during the spectral fitting. Error bars are 1σ . Models 2-3 and 5-6 have their power-law slope (kT_{bremss}) parameter held fixed at the 90% confidence value of models 1 and 4, respectively.

Table 2. Fraction of Featureless MC Spectra which produce single-energy-trial “lines” at 99% and 99.9% confidence between 0.4 and 1.5 keV

Model	>99% (1 z bin)	>99.9% (1 z bin)
1	0.79	0.14
2	0.80	0.14
3	0.77	0.15
4	0.80	0.16
5	0.75	0.14
6	0.82	0.16

Table 3. Fraction of Featureless MC Spectra which produce single- z -trial $\chi(z)$ at 99% and 99.9% confidence between $z = 1.88$ and $z = 2.40$

Model	$>99\%$ (1 z bin)	$>99.9\%$ (6 z bins)
1	0.16	0.013
2	0.22	0.026
3	0.20	0.017
4	0.25	0.014
5	0.21	0.012
6	0.23	0.017